A library for computing the filtered and non-filtered 3D Green's tensor associated with infinite homogeneous space and surfaces [☆],[☆☆]

Philippe Gay-Balmaz [*], Olivier J.F. Martin

Electromagnetic Fields and Microwave Electronics Laboratory, Swiss Federal Institute of Technology, ETH-Zentrum, ETZ, CH-8092 Zurich, Switzerland

Abstract

We describe a library to compute various types of Green's tensor for three-dimensional electromagnetic scattering calculations. This library includes the retarded and non-retarded (quasi-static) Green's tensors for infinite homogeneous space and the non-retarded Green's tensor associated with a surface. Both standard and filtered Green's tensor can be computed. Filtered Green's tensor can be used to accurately investigate high permittivity scatterers with the coupled-dipole approximation. © 2002 Elsevier Science B.V. All rights reserved.

PROGRAM SUMMARY

Title of program: LIBG3D

Catalogue identifier: ADPS

Program Summary URL: http://cpc.cs.qub.ac.uk/summaries/ADPS

Program obtainable from: CPC Program Library, Queen's University of Belfast, N. Ireland

Computer for which the program is designed and others on which it has been tested: Computers: SUN ULTRA 60 (ULTRASPARC II 360 MHz); *Installations:* 256 MB RAM

Operating systems or monitors under which the program has been tested: Solaris 2.7

Programming language used: Fortran 77

Memory required to execute with typical data: 208 KB

No. of bits in a word: 64

No. of processors used: 1

Nature of physical problem
Computation of the Green's tensor $\mathbf{G}(\mathbf{r}, \mathbf{r}')$, i.e. of the field radiated
at the observation point $\mathbf{r}$ by three orthogonal source dipoles located
at $\mathbf{r}'$. This dyadic is computed both for free space and for a surface in
the quasi-static limit. Further, the so-called filtered Green's tensor,
which increases the application range of the coupled-dipole approx-
imation to higher permittivity scatterers can also be computed [1].

Method of solution
Analytical expressions from the free space Green's tensor are com-
bined to obtain the electrostatic Green's tensor associated with a
surface. For the filtered Green's tensor, a spectral approach, with
integration in complex space is used [2,3].

References
[1] N.B. Piller, O.J.F. Martin, Increasing the performances of
    the coupled-dipole approximation: A spectral approach, IEEE
    Trans. Antennas Propag. 46 (1998) 1126–1137.
[2] P. Gay-Balmaz, O.J.F. Martin, Validity domain and limitation
    of non-retarded Green's tensor for electromagnetic scattering at
    surfaces, Opt. Comm. 184 (2000) 37–47.
[3] P. Gay-Balmaz, O.J.F. Martin, Electromagnetic scattering of
    high permittivity particles on a substrate, Appl. Optics (2001)
    (in press).

LONG WRITE-UP

1. Introduction

The Green's tensor $\mathbf{G}(\mathbf{r}, \mathbf{r}')$ plays a key role in computational electromagnetics, wherever an integral formulation is used [1–3]. This dyadic is, for example, utilized for computing the field scattered by dielectric objects in free space [4–6] or embedded in a stratified background [7]; or for investigating radiating structures such as patch antennas [8]. In both types of calculations, an integral formulation is used, leading to a very efficient numerical scheme where only the elements that differ from the background must be discretized. Like this, in the radiating structure case, only the metalizations on which the electric currents flow must be discretized. For the scattering calculation, only the scatterers must be discretized. In this way the number of unknowns remains quite limited, compared to other techniques such as finite differences time domain (FDTD) [9] or finite elements [10], where the entire geometry must be discretized. Another benefit of this integral formulation is the automatic and perfect fulfillment of the boundary conditions at the edge of the computation window, which are already included in the Green's tensor [6,11].

The library described in this paper can be used to compute the Green's tensor associated with an infinite homogeneous space and with a surface in the non-retarded (or quasi-static) limit. Analytical formulae exist for this dyadic and its implementation is straightforward. This is not the case for another class of Green's tensor that we recently introduced. This so-called filtered Green's tensor provides a much more accurate solution when high permittivity scatterers are at hand [12,13]. Unfortunately it is more difficult to compute and the primary purpose of our library is to provide an implementation for this filtered Green's tensor.

The underlying theory is briefly described in Section 2. The different subroutines in the library are described in Section 3 and test runs are presented in Section 4.

2. Theory

Many scattering problems can be successfully analyzed using the Fredholm equation of 2nd kind

$$\mathbf{E}(\mathbf{r}) = \mathbf{E}^0(\mathbf{r}) + \int_V d\mathbf{r}'\, \mathbf{G}(\mathbf{r}, \mathbf{r}') \cdot k_0^2\, \Delta\varepsilon(\mathbf{r}')\, \mathbf{E}(\mathbf{r}'), \tag{1}$$

for the electric field $\mathbf{E}(\mathbf{r})$ scattered by the three-dimensional (3D) scatterer of relative permittivity $\varepsilon(\mathbf{r})$ illuminated with the incident field $\mathbf{E}^0(\mathbf{r})$ [6,7]. In Eq. (1), $\Delta\varepsilon(\mathbf{r}')$ is the dielectric contrast between the scatterer and the surrounding medium. It is given by $\Delta\varepsilon(\mathbf{r}) = \varepsilon(\mathbf{r}) - \varepsilon_B$ where ε_B is the background permittivity. k_0 is the wavenumber in vacuum. The kernel $\mathbf{G}(\mathbf{r}, \mathbf{r}')$ in Eq. (1) is the Green's tensor associated with the background where the scatterer is placed. This dyadic takes the form

$$\mathbf{G}(\mathbf{r}, \mathbf{r}') = \begin{pmatrix} G_{xx} & G_{xy} & G_{xz} \\ G_{yx} & G_{yy} & G_{yz} \\ G_{zx} & G_{zy} & G_{zz} \end{pmatrix}, \tag{2}$$

and has a very simple physical interpretation: G_{ij} is the i-component of the electric field at the observation point $\mathbf{r}$ generated by an electric dipole located at $\mathbf{r}'$ and oriented along the j-axis.

The dyadic $\mathbf{G}(\mathbf{r}, \mathbf{r}')$ diverges for $\mathbf{r} = \mathbf{r}'$. Therefore, whenever both $\mathbf{r}$ and $\mathbf{r}'$ are inside the scatterer volume V, the principal value must be taken for the integral in Eq. (1) and the singularity of the Green's tensor must be treated separately, as described in Ref. [6]. Eq. (1) becomes then

$$\mathbf{E}(\mathbf{r}) = \mathbf{E}^0(\mathbf{r}) + \lim_{\delta V \to 0} \int_{V-\delta V} d\mathbf{r}'\, \mathbf{G}(\mathbf{r}, \mathbf{r}') \cdot k_0^2\, \Delta\varepsilon(\mathbf{r}')\, \mathbf{E}(\mathbf{r}') - \mathbf{L} \cdot \frac{\Delta\varepsilon(\mathbf{r})}{\varepsilon_B} \mathbf{E}(\mathbf{r}), \tag{3}$$

where the infinitesimal volume δV centred at the point $\mathbf{r}$ is used to exclude the singularity.

To solve Eq. (3) numerically, the volume of the scatterer is discretized into N cells. Introducing V_i and $\mathbf{r}_i$ for the volume, respectively the position of the centre of cell i, we can define $\mathbf{E}(\mathbf{r})|_{\mathbf{r} \in V_i} \approx \mathbf{E}_i = \mathbf{E}(\mathbf{r}_i)$ and $\Delta\varepsilon_i(\mathbf{r})|_{\mathbf{r} \in V_i} \approx \Delta\varepsilon_i = \Delta\varepsilon(\mathbf{r}_i)$. Like this Eq. (3) can be rewritten as a dense system of linear equations,

$$\mathbf{E}_i = \mathbf{E}_i^0 + \sum_{j=1,\, j \neq i}^N \mathbf{G}_{i,j}^B \cdot k_0^2\, \Delta\varepsilon_j\, \mathbf{E}_j V_j + \mathbf{M}_i \cdot k_0^2\, \Delta\varepsilon_i\, \mathbf{E}_i - \mathbf{L} \cdot \frac{\Delta\varepsilon_i}{\varepsilon_B} \mathbf{E}_i, \quad i = 1, \ldots, N, \tag{4}$$

with

$$\mathbf{M}_i = \lim_{\delta V \to 0} \int_{V_i - \delta V} d\mathbf{r}'\, \mathbf{G}^B(\mathbf{r}_i, \mathbf{r}'). \tag{5}$$

Different approximations can be found in the literature for the self-term $\mathbf{M}_i$ [14]. LIBG3D returns the value of $\mathbf{M}_i$ obtained by mapping the mesh i onto a sphere, as described in Ref. [6]. The source dyadic $\mathbf{L}$ depends on the exclusion volume shape and is tabulated in Refs. [6,15]. For completeness, it can also be obtained from LIBG3D.

In the next, we consider non-magnetic materials ($\mu = \mu_0$) and assume an $\exp(-i\omega t)$ time dependence.

2.1. Regular Green's tensor for an infinite homogeneous 3D background

Green's tensor $\mathbf{G}^B(\mathbf{r}, \mathbf{r}')$ for an infinite homogeneous 3D background medium ε_B is well known. In our notation, explained in [6], it is given by

$$\mathbf{G}^B(\mathbf{r}, \mathbf{r}') = \left(\mathbf{1} + \frac{ik_B R - 1}{k_B^2 R^2} \mathbf{1} + \frac{3 - 3ik_B R - k_B^2 R^2}{k_B^2 R^4} \mathbf{R}\mathbf{R} \right) \frac{\exp(ik_B R)}{4\pi R}. \tag{6}$$

In Eq. (6), $\mathbf{1}$ is the unit dyad, $R = |\mathbf{R}| = |\mathbf{r} - \mathbf{r}'|$ the relative distance between source and observation points and k_B the wave number in the background medium.

2.2. Non-retarded Green's tensor for an infinite homogeneous 3D background

For the quasi-static case, which can be used for low dimension systems, the Green's tensor associated with an infinite homogeneous 3D background medium is obtained from Eq. (6) with $k_B \to 0$ [13]. It is given by,

$$\mathbf{G}_{qs}^B(\mathbf{r}, \mathbf{r}') = \left(\frac{-1}{k_B^2 R^2} \mathbf{1} + \frac{3}{k_B^2 R^4} \mathbf{R}\mathbf{R} \right) \frac{1}{4\pi R}. \tag{7}$$

Note that the $1/R$ and $1/R^2$ terms in $\mathbf{G}^B$ have now disappeared in the electrostatic limit.

2.3. Non-retarded Green's tensor for a two-layers background

In Ref. [13] we derived the non-retarded (or quasi-static) Green's tensor for a two-layers background from the exact, retarded formulation.

In that case, the Green's tensor depends on the source-observer configuration (see Fig. 1). For $z \geqslant 0$, $z' < 0$ we have:

$$\mathbf{G}_{qs}(\mathbf{r}, \mathbf{r}') = \frac{2\varepsilon_2}{\varepsilon_1 + \varepsilon_2} \mathbf{G}_{qs}^2(\mathbf{r}, \mathbf{r}'). \tag{8}$$

For $z \geqslant 0$ and $z' \geqslant 0$ we have:

$$\mathbf{G}_{qs}(\mathbf{r}, \mathbf{r}') = \mathbf{G}_{qs}^2(\mathbf{r}, \mathbf{r}') \mp \frac{\varepsilon_1 - \varepsilon_2}{\varepsilon_1 + \varepsilon_2} \mathbf{G}_{qs}^2(\mathbf{r}, \mathbf{r}''). \tag{9}$$

In Eqs. (8) and (9), $\mathbf{G}_{qs}^2(\mathbf{r}, \mathbf{r}')$ is given by Eq. (7) with $k_B = k_2$. In Eq. (9) the minus sign, respectively the plus sign, refers to horizontal (x-, y-directed), respectively vertical (z-directed) sources. The vector $\mathbf{r}''$ determines the location of an image source as illustrated in Fig. 1(b).

For $z < 0$ and $z' < 0$ we have:

$$\mathbf{G}_{qs}(\mathbf{r}, \mathbf{r}') = \mathbf{G}_{qs}^1(\mathbf{r}, \mathbf{r}') \pm \frac{\varepsilon_1 - \varepsilon_2}{\varepsilon_1 + \varepsilon_2} \mathbf{G}_{qs}^1(\mathbf{r}, \mathbf{r}''). \tag{10}$$

And for $z < 0$ and $z' \geqslant 0$:

$$\mathbf{G}_{qs}(\mathbf{r}, \mathbf{r}') = \frac{2\varepsilon_1}{\varepsilon_1 + \varepsilon_2} \mathbf{G}_{qs}^1(\mathbf{r}, \mathbf{r}'). \tag{11}$$
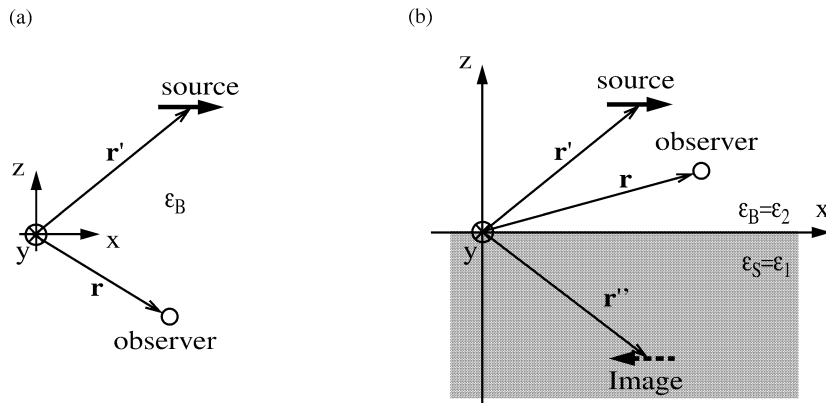

Fig. 1. Coordinates of the observer and source points located (a) inside an infinite homogeneous 3D background of permittivity ε_B and (b) inside a two-layers background made up of an upper layer of permittivity $\varepsilon_B = \varepsilon_2$ and a lower layer of permittivity $\varepsilon_S = \varepsilon_1$.

In Eqs. (10) and (11), $\mathbf{G}_{qs}^{1}(\mathbf{r}, \mathbf{r}')$ is given by Eq. (7) with $k_B = k_1$. In Eq. (10) the plus sign, respectively the minus sign, is associated with horizontal, respectively vertical sources.

2.4. Regular filtered Green's tensor for an infinite 3D background

Simple analytical formulae exist for the above discussed Green's tensors. This is not the case for the so-called filtered Green tensor, which we introduced in Ref. [16] to handle high permittivity scatterers. The filtering procedure is based on the sampling theory and is performed in Fourier space as described in detail in Ref. [16]. The interested reader is referred to that article for derivation details; we shall only give final results in the present paper.

The filtered Green's tensor for an infinite homogeneous medium takes the form:

$$\mathbf{G}^{F}(\mathbf{r}, \mathbf{r}') = \left(g^{F} + \frac{g'^{F}}{k_B^2 R} \right) \mathbf{1} + \left(\frac{-g'^{F}}{k_B^2 R^3} + \frac{g''^{F}}{k_B^2 R^2} \right) \mathbf{RR} + \frac{1}{3k_B^2} h^r (\mathbf{r} - \mathbf{r}_k), \tag{12}$$

with

$$h^r(\mathbf{r}) = \frac{\sin(k_F|\mathbf{r}|) - k_F|\mathbf{r}|\cos(k_F|\mathbf{r}|)}{2\pi^2|\mathbf{r}|^3}, \tag{13}$$

$$g^{F} = g^{B} - \frac{\alpha}{4\pi^2 R}, \tag{14}$$

$$g'^{F} = ik_B g^{B} - \frac{g^{B}}{R} + \frac{\alpha}{4\pi^2 R^2} - \frac{\alpha'}{4\pi^2 R}, \tag{15}$$

$$g''^{F} = -k_B^2 g^{B} - \frac{2ik_B g^{B}}{R} + \frac{2g^{B}}{R^2} - \frac{\alpha}{2\pi^2 R^3} + \frac{\alpha'}{2\pi^2 R^2} - \frac{\alpha''}{4\pi^2 R}. \tag{16}$$

In Eqs. (13)–(16), g^{B} is the scalar Green's function associated with an infinite homogeneous medium of permittivity ε_B. In the above equations

$$\alpha = \sin(k_B R)[\text{Ci}^+ - \text{Ci}^-] + \cos(k_B R)[\pi - \text{Si}^+ - \text{Si}^-], \tag{17}$$

$$\alpha' = k_B \sin(k_B R)[-\pi + \text{Si}^- + \text{Si}^+] + k_B \cos(k_B R)[\text{Ci}^+ - \text{Ci}^-] - \frac{2\sin(k_F R)}{R}, \tag{18}$$

$$\alpha'' = k_B^2 \sin(k_B R)[\text{Ci}^- - \text{Ci}^+] + k_B^2 \cos(k_B R)[\text{Si}^- + \text{Si}^+ - \pi] + \frac{2\sin(k_F R)}{R^2} - \frac{2k_F \cos(k_F R)}{R}, \tag{19}$$

and $\text{Ci}^{\pm} = \text{Ci}[(k_F \pm k_B)R]$, and $\text{Si}^{\pm} = \text{Si}[(k_F \pm k_B)R]$, where Ci and Si are cosine integral and sine integral. Parameter k_F depends on the mesh lattice and its optimal value has been derived in [16]: $k_F = \pi/\text{rmesh}$, where `rmesh` is the side of the mesh (the filtered coupled-dipole approximation relies implicitly on a cubic discretization mesh [16]).

2.5. Non-retarded filtered Green's tensor for an infinite 3D background

From Eq. (12) it is possible to derive a quasi-static approximation for the filtered Green's tensor, as explained in detail in Ref. [17]. This leads to

$$\mathbf{G}_{qs}^{F}(\mathbf{r}, \mathbf{r}') = \left(\frac{g_{qs}'^{F}}{k_B^2 R} \right) \mathbf{1} + \left(\frac{-g_{qs}'^{F}}{k_B^2 R^3} + \frac{g_{qs}''^{F}}{k_B^2 R^2} \right) \mathbf{RR} + \frac{1}{3k_B^2} h^r (\mathbf{r} - \mathbf{r}_k), \tag{20}$$

where

$$g_{qs}^{F} = g_{qs}^{B} - \frac{\alpha_{qs}}{4\pi^2 R}, \tag{21}$$

$$g_{qs}^{'F} = -\frac{g_{qs}^{B}}{R} + \frac{\alpha_{qs}}{4\pi^2 R^2} - \frac{\alpha_{qs}'}{4\pi^2 R}, \tag{22}$$

$$g_{qs}^{''F} = \frac{2g_{qs}^{B}}{R^2} - \frac{\alpha_{qs}}{2\pi^2 R^3} + \frac{\alpha_{qs}'}{2\pi^2 R^2} - \frac{\alpha_{qs}''}{4\pi^2 R}, \tag{23}$$

and

$$\alpha_{qs} = \pi - 2\mathrm{Si}(k_F R), \tag{24}$$

$$\alpha_{qs}' = -\frac{2\sin(k_F R)}{R}, \tag{25}$$

$$\alpha_{qs}'' = \frac{2\sin(k_F R)}{R^2} - \frac{2k_F \cos(k_F R)}{R}. \tag{26}$$

2.6. Non-retarded filtered Green's tensor for a two-layers background

The formulae for the non-retarded filtered Green's tensor associated with a two-layers background are identical to Eqs. (8)–(11), with the quasi-static Green's tensor replaced by the filtered Green's tensor given in Section 2.5.

3. Program description

In this section we describe all the procedures included in this library. The code consists of 8 subroutines plus a main program that can be used for test purposes.

3.1. Test program TESTG3D

The main program TESTG3D provides an example on how to call the different subroutines necessary for the calculations of the various Green's tensor types. In a first step, this program reads the input file DATA, where the type of Green's tensor must be specified by the user, by attributing a value to the variable ityp, as described in Table 1. On the second line of DATA, one gives the free-space wavelength wavel. Note that the wavelength determines all the units in the program (i.e. if wavel is given in nanometre, all dimensions are then implicitly in nanometres). The third line of DATA gives the background complex permittivity cepsBa $= \varepsilon_B$, as defined in Figs. 1(a) and 1(b). The next two lines concern the source and observation points, and must be written as x, y, z triplets. The next parameter of DATA is rmesh, which is used for the computation of the filtered Green's tensor. This parameter must be chosen smaller than the wavelength, typically $\frac{\lambda}{4}$ [16]. The last parameter is the permittivity of the surface cepsSu $= \varepsilon_S$; this parameter is defined in Fig. 1(b). Note that it is not used when the free space Green's tensor is computed.

Table 1
Value of the parameter ityp for the different Green's tensors of the library

ityp	Green's tensor
1	Regular Green's tensor for a homogeneous infinite background
2	Quasi-static Green's tensor for a homogeneous infinite background
3	Quasi-static Green's tensor for a surface
4	Regular filtered Green's tensor for an homogeneous infinite background
5	Quasi-static filtered Green's tensor for an homogeneous infinite background
6	Quasi-static filtered Green's tensor for a surface

Table 2 gives an example of DATA file for calculating the quasi-static Green's tensor ($\mathtt{ityp}=3$) associated with a two-layers medium with $\varepsilon_2 = 1$ and $\varepsilon_1 = 4$, for $\mathbf{r} = (5\ [\text{nm}], 0, 0)$ and $\mathbf{r}' = (0, 0, -25\ [\text{nm}])$, at a 500 [nm] vacuum wavelength.

The main program TESTG3D first calls an initialization subroutine called G3Dini, to initialize some parameters passed to the other subroutines via common. To include our library in a scattering code, it is mandatory that the initialization subroutine G3Dini is called first.

Then the main program calls the subroutine G3D, which returns the desired Green's tensor. Note that the subroutine G3Dini must only be called once for a given set of parameters wavel, cepsBa, cepsSu. The subroutine G3D can then be called as many times as one wishes for different $\mathbf{r}, \mathbf{r}'$ pairs. Finally TESTG3D calls G3DM and G3DL, which return the self term $\mathbf{M}$ and the source dyadic $\mathbf{L}$ used in Eq. (4) for the treatment of the singularity with the principal value.

Subroutines G3Dini, G3D, G3DM and G3DL are described in detail in the next sections.

3.2. Subroutine G3Dini

G3Dini is called from TESTG3D with CALL G3Dini(wavel,cepsBa,cepsSu), where wavel, cepsBa, cepsSu are defined in Table 2. Several parameters are defined in this subroutine and transmitted to other subroutines via common. The common has the following form:

```
common/G3Dcom/pi,cj,cepsB,cepsS,ckB,ckB2,ckS,ckS2
```

and the parameters are defined in Table 3 and Fig. 1. Note that cepsBa, respectively cepsSu are passed in the common as cepsB, respectively cepsS.

3.3. Subroutine G3D

G3D is called with G3D(ityp,r,rp,cG,rmesh). This routine returns the 3×3 matrix cG which includes the nine components of the selected Green's tensor as described in Eq. (2), for a source point located at $\mathtt{rp} = \mathbf{r}'$ and a field point at $\mathtt{r} = \mathbf{r}$. The parameter rmesh is only used if $\mathtt{ityp} = 4, 5$ or 6 (filtered cases). The routine G3D is divided into six parts corresponding to the six Green's tensor types defined in Table 1.

If $\mathtt{ityp} = 1$, subroutine G3D calls the subroutine G1, which calculates the regular Green's tensor associated with an homogeneous infinite background, as given by Eq. (6).

Table 2
Example of DATA file

3	! ityp (Green's tensor type)
500.d0	! wavel (wavelength)
(1.d0, 0.d0)	! cepsBa (permittivity of the background)
0.d0, 0.d0, −25.d0	! x',y',z' (coordinates of the source point)
5.d0, 0.d0, 0.d0	! x,y,z (coordinates of the observation point)
20.d0	! rmesh (mesh lattice)
(4.d0, 0.d0)	! cepsSu (permittivity of the surface)

Table 3
Parameters passed as common

$\mathtt{pi} = \pi$	$\mathtt{ckB} = k_B = \frac{2\pi}{\lambda}\sqrt{\varepsilon_B}$
$\mathtt{cj} = \sqrt{-1}$	$\mathtt{ckB2} = k_B^2$
$\mathtt{cepsB} = \varepsilon_B$	$\mathtt{ckS} = k_S = \frac{2\pi}{\lambda}\sqrt{\varepsilon_S}$
$\mathtt{cepsS} = \varepsilon_S$	$\mathtt{ckS2} = k_S^2$

For `itype = 2`, G3D calls the subroutine G1QS, which evaluates the non-retarded (quasi-static) Green's tensor associated with an infinite homogeneous background, which expression is given by Eq. (7).

If `itype = 3`, the quasi-static Green's tensor associated with a two-layers medium must be evaluated. As shown in Section 2.3, the expression for this Green's tensor depends on the source-observer configuration. A test over the source and observation points location is made and the Green's tensor evaluated by introducing Eq. (7) (whose value is given by subroutine G1QS) into Eqs. (8)–(11).

The value `ityp = 4` is selected for the calculation of the regular filtered Green's tensor associated with an homogeneous infinite background. In this case G3D calls the subroutine G2 which evaluates Eq. (12).

For `ityp = 5` (quasi-static filtered Green's tensor for an homogeneous infinite background), G3D calls the subroutine G2QS, which returns the value of Eq. (20).

Finally, for `ityp = 6`, the procedure is similar to the case `ityp = 3` and Eq. (20) (whose value is given by subroutine G2QS) is introduced into Eqs. (8)–(11).

3.3.1. Subroutine G1

Subroutine G1(cG,ck,ck2,dx,dy,dz,dr,dr2) returns the matrix cG corresponding to the regular Green's tensor associated with an homogeneous infinite background given by Eq. (6).

The value of ck depends on the value of parameter ityp. For ityp = 1, 2, 4 and 5, ck = ckB (see Table 3 and Fig. 1(a)) and ck2 = ckB2. For ityp = 3 and 6, the value of ck depends on the observer location. For an observation point inside the upper medium ($\mathbf{r} \geqslant 0$) (see Fig. 1(b)), ck = ckB and ck2 = ckB2) while for an observer inside the lower medium ($\mathbf{r} < 0$, ck = ckS and ck2 = ckS2, Fig. 1(b)).

Parameters dx, dy, dz, dr, dr2 are defined as follows dx = d$x = x - x'$, dy = d$y = y - y'$, dz = d$z = z - z'$, dr = d$r = (dx^2 + dy^2 + dz^2)^{1/2}$ and dr2 = dr^2, where (x, y, z), respectively (x', y', z') are the observer (field point), respectively source coordinates defined in Table 2.

3.3.2. Subroutine G1QS

Subroutine G1QS(cG,ck2,dx,dy,dz,dr,dr2) evaluates the quasi-static Green's tensor associated with an homogeneous infinite background given by Eq. (7). The parameters are the same as the one of routine G1.

3.3.3. Subroutine G2

Subroutine G2(cG,ck,ck2,dx,dy,dz,dr,dr2,rmesh) evaluates the regular filtered Green's tensor associated with an homogeneous infinite background given by Eq. (12). The parameter rmesh defines k_F which is used in the filtering process (Eqs. (12)–(19) and (20)–(26)).

3.3.4. Subroutine G2QS

Subroutine G2QS(cG,ck2,dx,dy,dz,dr,dr2,rmesh) calculates the quasi-static filtered Green's tensor associated with an homogeneous infinite background given by Eq. (20). It has the same parameters as subroutine G2.

3.4. Subroutine G3DM

Subroutine G3DM(ityp,r,cM,rmesh) returns the 3×3 matrix cM associated with the self-term **M** as defined by Eq. (5). The parameters ityp,r and rmesh) have been defined in Section 3.3.

3.5. Subroutine G3DL

Subroutine G3DL(ityp,r,cL) returns the 3×3 matrix cL corresponding to the source dyadic **L** which enters in Eq. (4) for the singularity of Green's dyadic.

4. Test run

For the test run we consider the input file DATA given in Section 3.1 (see Table 2). In this file we select in turn the six different values of ityp. For ityp = 1, 2, 4 and 5, the background is an infinite homogeneous medium with permittivity $\varepsilon_B = 1$. For ityp = 3 and 6, the background consists of a two-layers medium with upper, respectively lower permittivity $\varepsilon_B = \varepsilon_2 = 1$, respectively $\varepsilon_S = \varepsilon_1 = 4$. For these two configurations of the
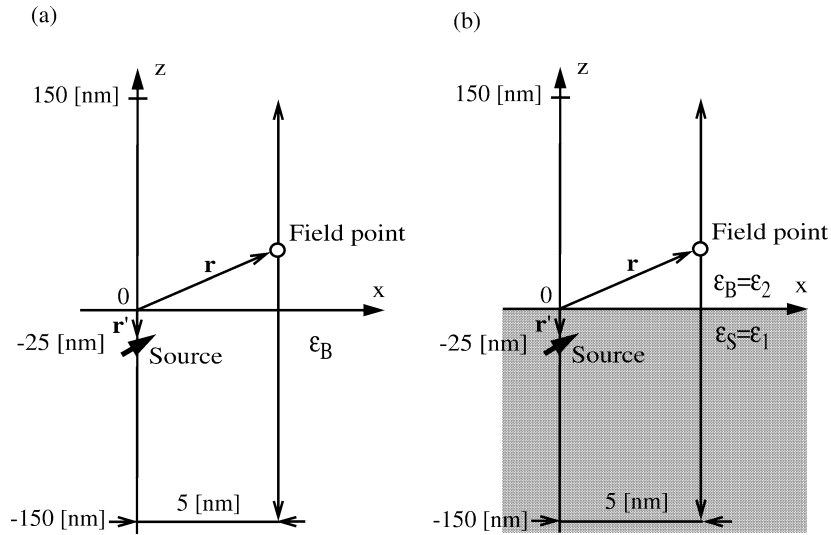

Fig. 2. (a) Infinite homogeneous medium and (b) two-layers medium with a source located at $x' = y' = 0$ [nm], $z' = -25$ [nm]. The fields displayed in Figs. 3 and 4 are calculated along the vertical segment of line defined in the figure ($x' = 5$ [nm], $y' = 0$ [nm], $z' = -150\ldots150$ [nm]).
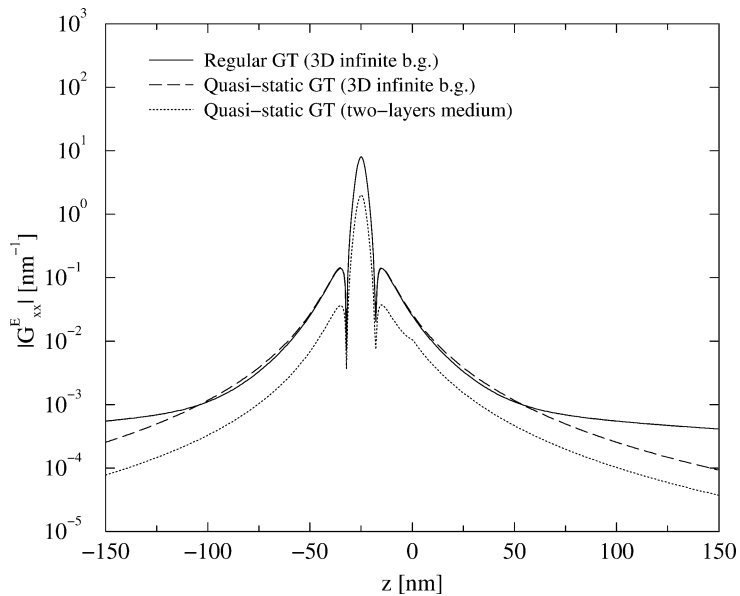

Fig. 3. Rigorous and quasi-static xx-component of the Green's tensor for the geometry depicted in Fig. 2(a) and quasi-static xx-component of the Green's tensor for the geometry depicted in Fig. 2(b).
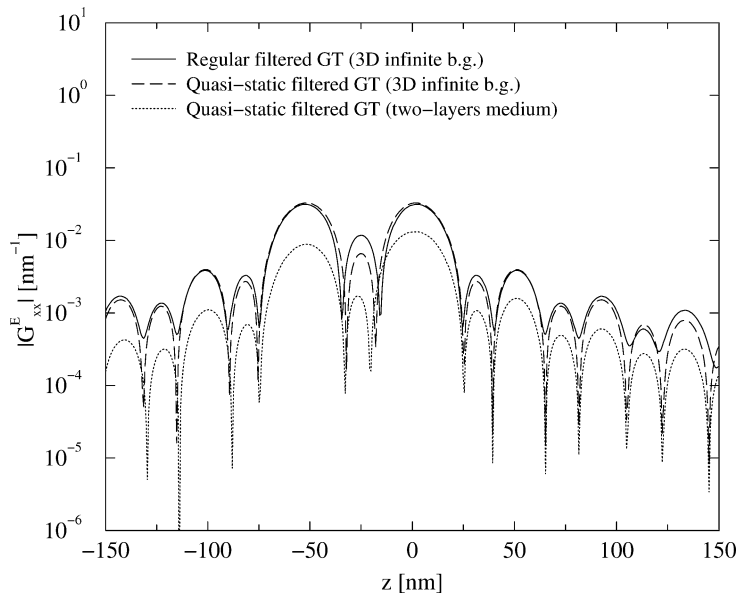
Fig. 4. Rigorous and quasi-static filtered xx-component of the Green's tensor for the geometry depicted in Fig. 2(a) and quasi-static filtered xx-component of the Green's tensor for the geometry depicted in Fig. 2(b).

background, we consider a point source located at $x' = y' = 0$ [nm], $z' = -25$ [nm], and we compute the Green's tensor components along the z-axis, from $z = -150$ [nm] to $z = 150$ [nm], at a short transverse distance of the source ($x = 5$ [nm], $y = 0$ [nm], see Fig. 2). The vacuum wavelength is $\lambda = 500$ [nm].

In Fig. 3, we show the xx-component (1) of the regular Green's tensor for an infinite homogeneous background (`ityp = 1`), (2) of the quasi-static Green's tensor for the same background (`ityp = 2`), (3) of the quasi-static Green's tensor associated with a surface (`ityp = 3`).

In Fig. 4 we show the results for the filtered cases, i.e. setting in turn `ityp = 4`, `ityp = 5`, `ityp = 6`, in the `DATA` file.

References

[1] L.B. Felsen, N. Marcuvitz, Radiation and Scattering of Waves, IEEE Press, New York, 1994.
[2] C.-T. Tai, Dyadic Green Function in Electromagnetic Theory, IEEE Press, New York, 1994.
[3] J.D. Jackson, Classical Electrodynamics, 3rd edn., Wiley, New York, 1999.
[4] B.T. Draine, P.J. Flatau, J. Opt. Soc. Amer. A 11 (1994) 1491–1499.
[5] P.J. Flatau, Opt. Lett. 22 (1997) 1205–1207.
[6] O.J.F. Martin, N.B. Piller, Phys. Rev. E 58 (1998) 3909–3915.
[7] M. Paulus, O.J.F. Martin, J. Opt. Soc. Amer. A 18 (2001) 854–861.
[8] L. Barlatey, J.R. Mosig, T. Sphicopoulos, IEEE Trans. Antennas Propag. 38 (1990) 608–615.
[9] A. Taflove, Computational Electrodynamics, the FDTD Method, Artech House, Boston, 1995.
[10] J.L. Volakis, A. Chatterjee, L.C. Kempel, J. Opt. Soc. Amer. A 11 (1994) 1422–1433.
[11] M. Paulus, P. Gay-Balmaz, O.J.F. Martin, Phys. Rev. E 62 (2000) 5797–5807.
[12] N.B. Piller, O.J.F. Martin, Opt. Comm. 150 (1998) 1–6.
[13] P. Gay-Balmaz, O.J.F. Martin, Opt. Comm. 184 (2000) 37–47.
[14] G.H. Goedecke, S.G. O'Brien, Appl. Opt. 27 (1988) 2431–2438.
[15] A.D. Yaghjian, Proc. IEEE 68 (1980) 248–263.
[16] N.B. Piller, O.J.F. Martin, IEEE Trans. Antennas Propag. 46 (1998) 1126–1137.
[17] P. Gay-Balmaz, O.J.F. Martin, Appl. Opt. 40 (2001) 4562–4568.